



# MrgprC11<sup>+</sup> sensory neurons mediate glabrous skin itch

Haley R. Steele<sup>a</sup>, Yanyan Xing<sup>a</sup>, Yuyan Zhu<sup>a</sup>, Henry B. Hilley<sup>a</sup>, Katy Lawson<sup>a</sup>, Yeseul Nho<sup>a</sup>, Taylor Niehoff<sup>a</sup>, and Liang Han<sup>a,1</sup>

<sup>a</sup>School of Biological Sciences, Georgia Institute of Technology, Atlanta, GA 30332

Edited by Jeremy Nathans, Johns Hopkins University School of Medicine, Baltimore, MD, and approved March 2, 2021 (received for review November 2, 2020)

**Itch arising from glabrous skin (palms and soles) has attracted limited attention within the field due to the lack of methodology. This is despite glabrous itch arising from many medical conditions such as plantar and palmar psoriasis, dyshidrosis, and cholestasis. Therefore, we developed a mouse glabrous skin behavioral assay to investigate the contribution of three previously identified pruriceptive neurons in glabrous skin itch. Our results show that MrgprA3<sup>+</sup> and MrgprD<sup>+</sup> neurons, although key mediators for hairy skin itch, do not play important roles in glabrous skin itch, demonstrating a mechanistic difference in itch sensation between hairy and glabrous skin. We found that MrgprC11<sup>+</sup> neurons are the major mediators for glabrous skin itch. Activation of MrgprC11<sup>+</sup> neurons induced glabrous skin itch, while ablation of MrgprC11<sup>+</sup> neurons reduced both acute and chronic glabrous skin itch. Our study provides insights into the mechanisms of itch and opens up new avenues for future glabrous skin itch research.**

itch | Mrgprs | glabrous skin

Chronic itch is a debilitating disease that arises from a multitude of etiologies. It is the most common reason for visiting the dermatologist and has few effectual treatments (1, 2). Although itch sensation can arise from any area of the skin, itchy palms and soles (hairless glabrous skin) are considered the most debilitating and are associated with many dermatological and systemic conditions (3–5). A few examples include palmoplantar pustulosis (or palmar and plantar psoriasis), a chronic skin disease characterized by inflamed scaly skin and intense itch on the palms and soles that is reported to affect 0.01 to 0.05% of the US population (4); dyshidrosis, a skin condition causing itchy blisters to develop only on the palm and soles that results in an estimated 200,000 US cases per year (5); and cholestatic itch, an intense itching sensation felt in the limbs, and particularly the palms and soles of feet, frequently reported with hepatobiliary disorders (3). In recent years, considerable progress has been made in our understanding of itch with the identification of key molecules and neuronal populations mediating itch in both the peripheral and central nervous system (2, 6). However, the majority of established itch behavioral assays are performed with pruritogens applied to the hairy skin including the back, cheek, and hindlimb (7). Since hairy and glabrous skin are anatomically and physiologically distinct and are innervated by different cutaneous nerves (8, 9), it is unclear whether different mechanisms are employed for itch arising from the two types of skin.

Recent functional studies and single-cell RNA-sequencing analysis have characterized three subtypes of itch-sensing neurons in the dorsal root ganglia (10–14). Two of them are labeled by MrgprA3 and MrgprD, respectively, both of which are members of the Mrgpr (mas-related G protein-coupled receptor) itch receptor family (15). MrgprA3<sup>+</sup> neurons can respond to multiple pruritogens and play a key role in both acute and chronic itch (16–19). MrgprD<sup>+</sup> neurons mediate β-alanine-induced itch and are defined as itch-sensing neurons (20). Additionally, Sst<sup>+</sup>/Nppb<sup>+</sup> neurons express a distinct array of itch receptors and are key mediators for mast cell-induced itch (12, 21). However, it is unknown whether these defined pruriceptive neuronal populations project to the glabrous skin and whether they play a role in glabrous skin itch.

In this study, we analyzed skin innervation patterns of three subtypes of itch-sensing neurons and found that MrgprA3<sup>+</sup> neurons only sparsely innervate the glabrous skin. This result raises the question if the itch mechanisms in hairy skin and glabrous skin are different. This is a critical question, as different itch mechanisms implies the need for different clinical treatment strategies. Therefore, to investigate the mechanisms of glabrous skin itch, we developed a mouse behavioral assay to examine itch sensation arising from the glabrous skin of the plantar hindpaw. Using this itch assay, combined with genetic, physiological, and chemogenetic approaches, we demonstrate that glabrous skin itch is mainly mediated by MrgprC11<sup>+</sup> neurons, but not MrgprA3<sup>+</sup> or MrgprD<sup>+</sup> neurons.

## Results

**MrgprC11<sup>+</sup> and MrgprD<sup>+</sup> Neurons, Not MrgprA3<sup>+</sup> Neurons, Densely Innervate Glabrous Skin.** To identify which neuronal populations might mediate glabrous skin itch, we began examining the skin innervation of three previously identified itch-sensing neurons: MrgprA3<sup>+</sup>, MrgprC11<sup>+</sup>, and MrgprD<sup>+</sup> neurons. The skin nerves were visualized by the Cre-dependent expression of tdTomato. *MrgprA3<sup>GFP-Cre</sup>* and *MrgprD<sup>CreERT2</sup>* lines were previously generated (19, 22), while we generated a *MrgprC11<sup>CreERT2</sup>* line (23). We collected cross-sections of *MrgprA3<sup>tdTomato</sup>*, *MrgprC11<sup>tdTomato</sup>*, and *MrgprD<sup>tdTomato</sup>* mice hindpaws in the center of the walking pads. Similar to MrgprA3<sup>+</sup> and MrgprD<sup>+</sup> fibers (19, 24), MrgprC11<sup>+</sup> fibers are free nerve endings terminating in the superficial skin surface (Fig. 1A). Although MrgprA3<sup>+</sup> nerves were observed in the hindpaw glabrous skin, their innervation is sparse. Their fiber density in the hindpaw glabrous skin is much

## Significance

Chronic itch, associated with dermatologic or systemic diseases, is challenging to treat and significantly affects quality of life. In the past several decades, significant progress has been made to help us understand the mechanisms of itch. Due to the ease of application and analysis, all animal itch behavioral assays utilize pruritogens administered to the hairy skin. However, itch occurs to both hairy and hairless glabrous skin. Many medical conditions such as plantar and palmar psoriasis, dyshidrosis, and cholestasis mainly evoke itch in glabrous skin. We here present evidence demonstrating that distinct neuronal populations are responsible for mediating hairy and glabrous skin itch. This study advanced our understanding of itch and will have significant impact on the clinical treatment of itch.

Author contributions: L.H. designed research; H.R.S., Y.X., Y.Z., H.B.H., K.L., Y.N., T.N., and L.H. performed research; H.R.S., Y.X., Y.Z., H.B.H., Y.N., T.N., and L.H. analyzed data; and H.R.S. and L.H. wrote the paper.

The authors declare no competing interest.

This article is a PNAS Direct Submission.

Published under the PNAS license.

<sup>1</sup>To whom correspondence may be addressed. Email: lhan41@gatech.edu.

This article contains supporting information online at <https://www.pnas.org/lookup/suppl/doi:10.1073/pnas.2022874118/-DCSupplemental>.

Published April 5, 2021.

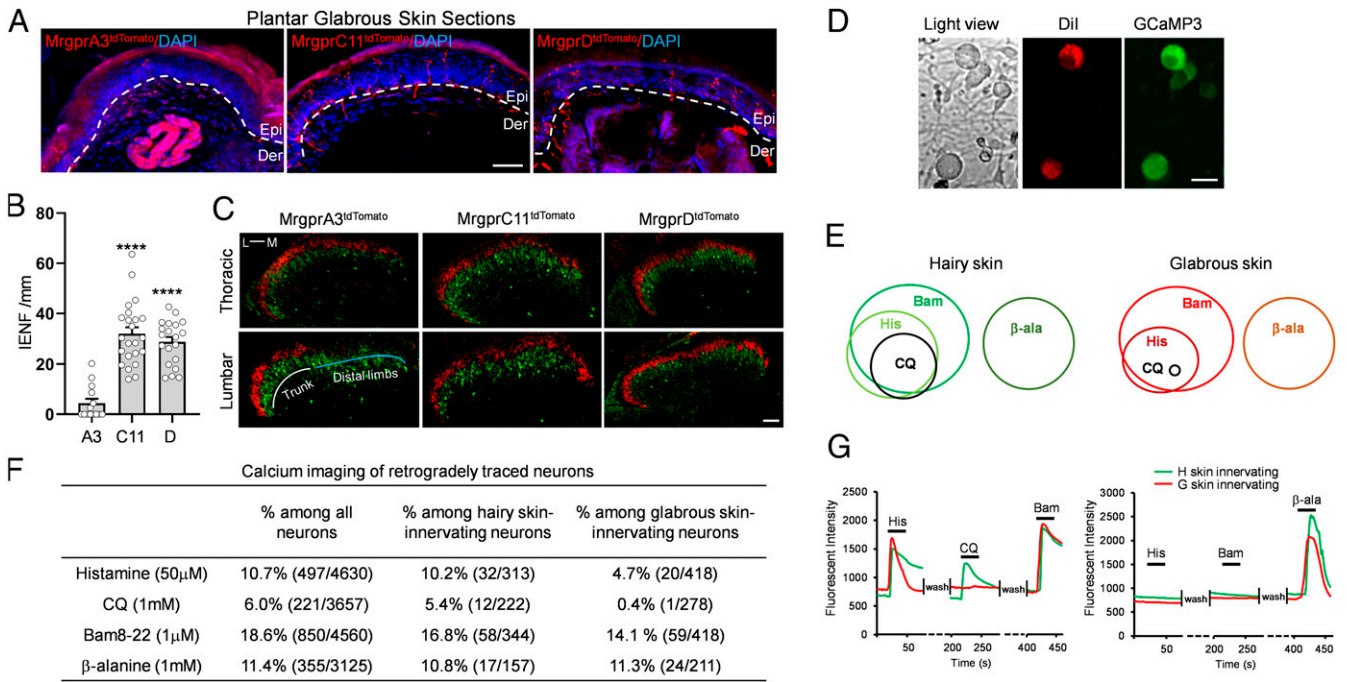


**Fig. 1.** MrgprC11<sup>+</sup> and MrgprD<sup>+</sup> neurons, not MrgprA3<sup>+</sup> neurons, densely innervate glabrous skin. (A) Plantar hindpaw glabrous skin sections from adult *MrgprA3<sup>GFP-Cre</sup>, ROSA26<sup>tdTomato</sup>*, *MrgprC11<sup>CreERT2</sup>, ROSA26<sup>tdTomato</sup>*, and *MrgprD<sup>CreERT2</sup>, ROSA26<sup>tdTomato</sup>* mice showing MrgprA3<sup>+</sup>, MrgprC11<sup>+</sup>, and MrgprD<sup>+</sup> nerves labeled by tdTomato fluorescence. Dashed lines indicate the boundary between the epidermis and dermis layers. (Scale bar: 50  $\mu$ m.) (B) The MrgprA3<sup>+</sup>, MrgprC11<sup>+</sup>, and MrgprD<sup>+</sup> intraepidermal nerve fiber (IENF) density in hindpaw plantar glabrous skin ( $n = 14$  to 23 sections from 3 mice were used for each genotype). Data are parametric and presented as mean  $\pm$  SEM ( $***P < 0.0001$  according to a one-way ANOVA test). (C) Spinal cord sections from the thoracic and lumbar regions of adult *MrgprA3<sup>GFP-Cre</sup>, ROSA26<sup>tdTomato</sup>*, *MrgprC11<sup>CreERT2</sup>, ROSA26<sup>tdTomato</sup>*, and *MrgprD<sup>CreERT2</sup>, ROSA26<sup>tdTomato</sup>* mice showing the central terminals of the sensory neurons labeled by tdTomato fluorescence. (Scale bar: 50  $\mu$ m.) All figures are presented with lateral side of the spinal cord to the left. L, lateral; M, medial. (D) Representative light and fluorescent view images of cultured DRG sensory neurons isolated from *Pirt<sup>GCaMP3</sup>* mice injected with retrograde tracer Dil. All four neurons in the view express GCaMP3, and two of them are labeled by Dil. (Scale bar: 25  $\mu$ m.) (E) Venn diagram illustrating the relative ratio of Dil-labeled glabrous skin-innervating neurons (lumbar DRGs) and hairy skin-innervating neurons (thoracic DRGs) that responded to each pruritogen. The sizes of the circles are proportional to the sizes of the cell populations. (F) Table displaying the percentage of neurons responded to each pruritogen in glabrous skin and hairy skin-innervating neurons labeled by Dil. The numbers of neurons analyzed are shown in parentheses. Cells from three mice were pooled together for analysis of each pruritogen. According to a  $\chi^2$  test, there is a significant difference in chloroquine response between glabrous and hairy skin cells ( $P = 0.0028$ ). (G) Representative traces evoked by histamine, chloroquine, Bam8-22, and  $\beta$ -alanine in hairy skin- and glabrous skin-innervating neurons.

lower than that of MrgprC11<sup>+</sup> and MrgprD<sup>+</sup> neurons (Fig. 1 A and B).

We next examined the central innervation of those neurons in the spinal cord dorsal horn. Central projections for all three neuronal types coterminated with IB4<sup>+</sup> fibers in the spinal lamina II<sub>middle</sub>, dorsal of PKC $\gamma$  lamina, and ventral to CGRP<sup>+</sup> lamina (Fig. 1C and SI Appendix, Fig. S1A). The central projections of dorsal root ganglion (DRG) sensory neurons are somatotopically organized in the dorsal horn of the spinal cord. Lumbar DRG sensory neurons innervating the trunk and proximal limb restrict their central projections to the lateral side of the lumbar spinal segments, while those innervating the distal limbs (containing both hairy and glabrous skin) project to the medial lumbar spinal cord (8, 25–27). Both MrgprC11<sup>+</sup> and MrgprD<sup>+</sup> neurons at the lumbar level showed complete medial-to-lateral innervation (Fig. 1C), suggesting that they densely innervate both trunk and limbs. However, MrgprA3<sup>+</sup> neurons at the lumbar level exhibited very sparse central innervation within the medial spinal cord despite PKC $\gamma$  costaining demonstrating the intact morphology of the spinal cord sections (Fig. 1C), suggesting that MrgprA3<sup>+</sup> neurons sparsely innervate the distal limbs. This is consistent with the limited MrgprA3<sup>+</sup> nerves we observed in the hindpaw glabrous skin (Fig. 1A). At the thoracic level, all three neuronal types had complete medial-to-lateral innervation (Fig. 1C).

We then performed retrograde tracing to label both hairy skin- and glabrous skin-innervating neurons and examine their physiological

properties. We injected neuronal tracer DiI into the plantar hindpaws or back hairy skin of *Pirt<sup>GCaMP3</sup>* mice (28) and performed calcium imaging with dissociated sensory neurons innervating the injected areas 1 wk later (Fig. 1D). We examined the percentage of neurons among hairy skin-innervating, glabrous skin-innervating, or all sensory neurons that responded to the MrgprA3 agonist chloroquine, MrgprC11 agonist Bam8-22, MrgprD agonist  $\beta$ -alanine, and histamine (Fig. 1E–G). Both hairy skin- and glabrous skin-innervating neurons showed strong responses to histamine, Bam8-22, and  $\beta$ -alanine (Fig. 1E–G). The majority of the histamine-sensitive neurons also responded to Bam8-22. This is consistent with the dense innervation of MrgprC11<sup>+</sup> neurons and MrgprD<sup>+</sup> neurons in both hairy and glabrous skin. Similar to previous reports (18, 29), 6.0% (221 of 3,657) of dissociated sensory neurons responded to chloroquine. We also observed that 5.4% (12 of 222) of hairy skin-innervating neurons responded to chloroquine. However, only 0.4% (1 of 278) of glabrous skin-innervating neurons exhibited calcium responses to chloroquine, consistent with the fact that MrgprA3<sup>+</sup> neurons sparsely innervate plantar hindpaw. Therefore, combining genetic axonal labeling and retrograde tracing, our results suggest MrgprC11<sup>+</sup> and MrgprD<sup>+</sup> neurons, but not MrgprA3<sup>+</sup> neurons, as candidates for mediating glabrous skin itch.

**MrgprC11<sup>+</sup> Neurons Represent a Unique Subpopulation of Nociceptors that Label the Majority of MrgprA3<sup>+</sup> and Nppb<sup>+</sup> Itch-Sensing Neurons.** Previous studies have reported the cellular features of MrgprD<sup>+</sup>

neurons in detail (22, 24). Here we performed molecular characterization of *MrgprC11*<sup>+</sup> neurons using immunostaining and RNAscope in situ hybridization. Consistent with a previous report (30), we found that *MrgprC11* is highly expressed during the early postnatal stage (57.0% at postnatal day [P] 0; 1,712 of 3,002). As the mice age, the percentage of *MrgprC11*<sup>+</sup> neurons declines until becoming stable around P20 (*SI Appendix, Fig. S1 B–D*). In adult lumbar DRG, *MrgprC11* was detected in 17.6% (642 of 3,645) of sensory neurons. They are of small diameter (average  $18.7 \pm 0.65 \mu\text{m}$ ; *SI Appendix, Fig. S1E*) and negative for myelinated neuron marker neurofilament 200kD (NF200; 0%, 0 of 505; Fig. 2A). The majority of *MrgprC11*<sup>+</sup> neurons express calcitonin gene-related peptide (CGRP; 79.5%, 307 of 386; Fig. 2B). About half of the *MrgprC11*<sup>+</sup> neurons are also labeled by TRPV1 (57.0%, 401 of 704), substance P (49.4%, 239 of 484), and IB4 (46.6%, 96 of 206; Fig. 2 C–E).

Interestingly, *MrgprA3*<sup>+</sup> neurons are a subset of *MrgprC11*<sup>+</sup> neurons. Almost all (95.2%, 139 of 146) of the *MrgprA3*<sup>+</sup> neurons express *MrgprC11* (Fig. 2I). Minimal overlap was observed between *MrgprC11*<sup>+</sup> and *MrgprD*<sup>+</sup> neurons (Fig. 2F). About 18.5% (61 of 330) of *MrgprC11*<sup>+</sup> neurons are expressing *MrgprD*. Very few *MrgprC11*<sup>+</sup> neurons express lysophosphatidic acid receptor (*Lpar3*; 0.9%, 2 of 234; Fig. 2G), an itch receptor highly expressed in *MrgprD*<sup>+</sup> neurons (12). Results of calcium imaging analysis of skin-innervating neurons (Fig. 1E) or neurons isolated from all spinal levels (*SI Appendix, Fig. S2 A and B*) are consistent with the receptor expression pattern. The majority of chloroquine-sensitive neurons (89.6%) responded to Bam8-22. We did not observe any overlap between  $\beta$ -alanine-sensitive neurons and Bam8-22-sensitive neurons. About half of the serotonin-sensitive neurons (48.3%), half of the capsaicin-sensitive neurons (43.6%), and most histamine-sensitive neurons (75.4%) also responded to Bam8-22 (Fig. 1E and *SI Appendix, Fig. S2 A and B*).

*Nppb*<sup>+</sup>/*Sst*<sup>+</sup> neurons have been identified as itch-sensing neurons and express multiple itch receptors (12, 21). We performed triple-label in situ hybridization to examine if *Nppb*<sup>+</sup> neurons express *MrgprA3* and *MrgprC11* (Fig. 2J). The results showed that *MrgprC11*, *MrgprA3*, and *Nppb* are expressed in 18.1%, 6.6%, and 7.3% of total DRG neurons, respectively. Consistent with the previous study (21), the expression of *MrgprA3* and *Nppb* are largely nonoverlapping. However, we found that the majority (60.0%, 27 of 45) of *Nppb*<sup>+</sup> neurons express *MrgprC11* (Fig. 2J). *Cyslr2* mediates LTC<sub>4</sub>-induced itch and is specifically expressed in *Nppb*<sup>+</sup> neurons (21). Most *Cyslr2*<sup>+</sup> neurons (61.1%, 140 of 229) also express *MrgprC11* (Fig. 2H). These data suggest that the expression of *MrgprC11* labels two pruriceptive sensory neuron populations: *MrgprA3*<sup>+</sup> neurons and *Nppb*<sup>+</sup>/*Sst*<sup>+</sup> neurons.

**Biting Behavior Directed to the Plantar Hindpaw Indicate Itch.** Mice hindpaw behaviors such as withdrawal, flinching, guarding, and licking have been well characterized as nocifensive behaviors indicating pain (31–33). Limited studies have been performed in the field to examine itch sensation arising from the hindpaw. Imamachi et al. suggested licking behavior after intraplantar injection of pruritogens 5-HT and endothelin-1 (34). However, other groups observed strong biting behaviors after 5-HT injection into the medial malleolus region of the hindpaw or dry skin treatment of the hindpaw (35–38). Biting was also observed when pruritogens were delivered to the calf of the hind leg, since this is the only way for mice to generate mechanical force to relieve itch (7). Since these previous studies were focusing on the whole hindpaw, including the dorsal hairy and plantar skin (7, 35–37), we ask if mice exhibit stereotypical behaviors in response to itch arising from glabrous skin. We analyzed behavioral responses after intraplantar injection of pruritogen histamine and algogen capsaicin. Only 4  $\mu\text{L}$  of chemical was delivered to avoid diffusion to the hairy side of the paw. The animals were recorded

for 10 min by a high-resolution camcorder, and videos were analyzed in slow motion to differentiate behavioral responses. We did not observe any significant behaviors 10 min after any chemical injection (Fig. 3 and *SI Appendix, Fig. S3 D and E*). Capsaicin injection induced typical licking characterized by long, slow head movement and visible tongue (Fig. 3 D–F). However, histamine induced typical biting characterized by pulling on the toes or scraping with their incisors, fast short head movement, and the absence of tongue (Fig. 3 A–C and *Movies S1–S4*). We then placed mice on a  $-2^\circ\text{C}$  cold plate to examine cold-induced pain. The animals also displayed significant licking behavior, but not biting (Fig. 3 G–I). These data suggest mice exhibit biting in response to itch arising from glabrous skin. Mice also exhibit significant flinching and guarding behaviors after both histamine and capsaicin injection. These results indicate that flinching and lifting/guarding behaviors represent nocifensive responses to noxious stimuli and are not good criteria to differentiate pain and itch sensation (*SI Appendix, Fig. S3 F–I*). We categorized the above behaviors in regard to total time (Fig. 3) and total numbers of episodes (*SI Appendix, Fig. S2 A–C*) and found that the data were consistent regardless of quantification method. We chose to use total time in all following tests since it better presents the dose-dependent effect of both histamine- and capsaicin-induced responses. To confirm that the injected chemicals did not diffuse into the hairy side of the hindpaw, we performed intradermal injections with saline mixed with trypan blue into glabrous skin. The blue color was restricted within the glabrous skin side (Fig. 3J).

It is well known that mice exhibit frequent grooming behavior toward their hindpaw. Indeed, our saline-injected control groups showed an average of  $2.29 \pm 0.57$  s background licking in 10 min. However, background biting behavior is rare (average  $0.30 \pm 0.16$  s). These data suggest that biting is not a grooming behavior and is instead a nocifensive behavior induced by itch sensation.

We next examined a glabrous skin allergic contact dermatitis model using squaric acid dibutylester (SADBE) (38). The treatment induced dryness, redness, and scabbing of the glabrous side of the hindpaws (Fig. 3 K and L). Since mice exhibited baseline grooming behavior, we presented the results as the percentage of the baseline to clearly show behavioral changes (Fig. 3M). Robust biting started to be observed  $\sim 5$  d into the hindpaw SADBE treatments. Significant biting was observed on day 17. We did not observe a significant increase in licking behavior. In summary, our results from both acute and chronic itch models suggest that biting behavior directed to the plantar hindpaw indicates itch sensation arising from the glabrous skin.

**Activation of *MrgprC11*<sup>+</sup> Neurons Induces Itch in Glabrous Skin.** We employed a Cre-dependent chemogenetic approach to examine if the activation of *MrgprA3*<sup>+</sup>, *MrgprD*<sup>+</sup>, or *MrgprC11*<sup>+</sup> neurons induces itch sensation in glabrous skin. We confirmed the expression of *Dreadd* within *MrgprA3*<sup>+</sup> and *MrgprD*<sup>+</sup> neurons using in situ hybridization (*SI Appendix, Fig. S4 A and B*) and within *MrgprC11*<sup>+</sup> neurons using immunostaining (*SI Appendix, Fig. S4C*). Clozapine N-oxide (CNO) injection to the nape of the neck skin induced robust scratching behavior in *MrgprA3*<sup>DREADD</sup>, *MrgprD*<sup>DREADD</sup>, and *MrgprC11*<sup>DREADD</sup>, demonstrating the functionality of the chemogenetic system (*SI Appendix, Fig. S4D*). CNO injection to the cheek hairy skin of those mice also induced strong scratching, but not wiping, confirming that *MrgprA3*<sup>+</sup>, *MrgprD*<sup>+</sup>, and *MrgprC11*<sup>+</sup> nerves in the hairy skin mediate itch sensation (*SI Appendix, Fig. S4 E and F*). However, CNO injection to the glabrous skin of the hindpaw did not produce any significant response in *MrgprA3*<sup>DREADD</sup> or *MrgprD*<sup>DREADD</sup> mice compared to *ROSA26*<sup>DREADD</sup> control littermates (Fig. 4 A–C). In contrast, we found *MrgprC11*<sup>DREADD</sup> mice exhibited robust biting when injected with CNO. These data suggest that *MrgprC11*<sup>+</sup> neurons mediate glabrous skin itch sensation. Increased licking

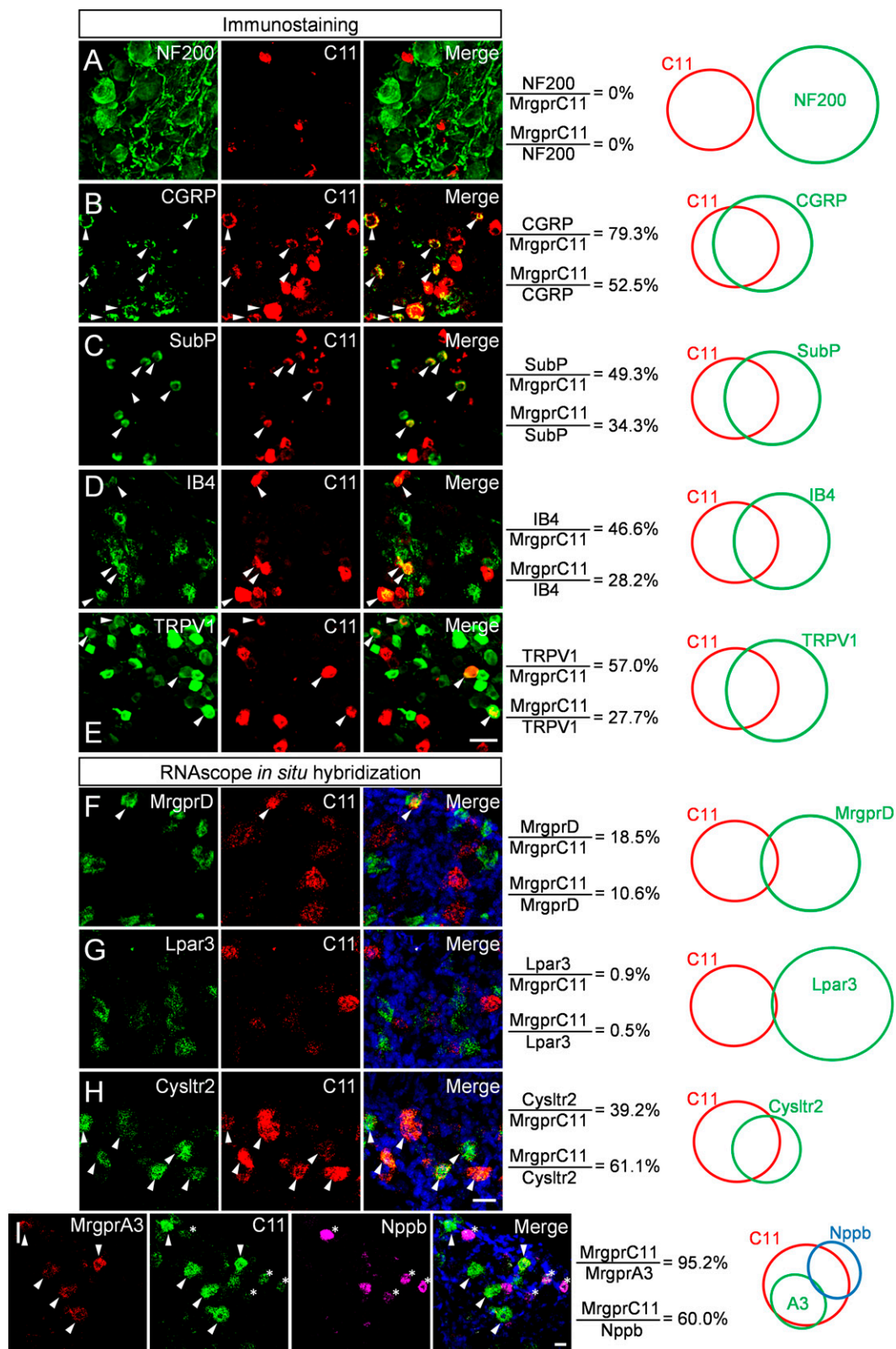


**Fig. 2.** Molecular characterization of MrgprC11<sup>+</sup> neurons. (A–E) Lumbar DRG sections from adult WT mice stained with the indicated markers. (Scale bar: 50 μm.) (F–I) RNAscope fluorescent *in situ* hybridization detecting indicated markers. Arrows indicate the cells expressing both markers. In I, arrows indicate that cells coexpress MrgprA3 and MrgprC11. Stars indicate that cells coexpress Nppb and MrgprC11. Venn diagrams on the right of each panel illustrate the relative expression patterns. The sizes of the circles are proportional to the sizes of the cell populations. (Scale bar: 25 μm.)

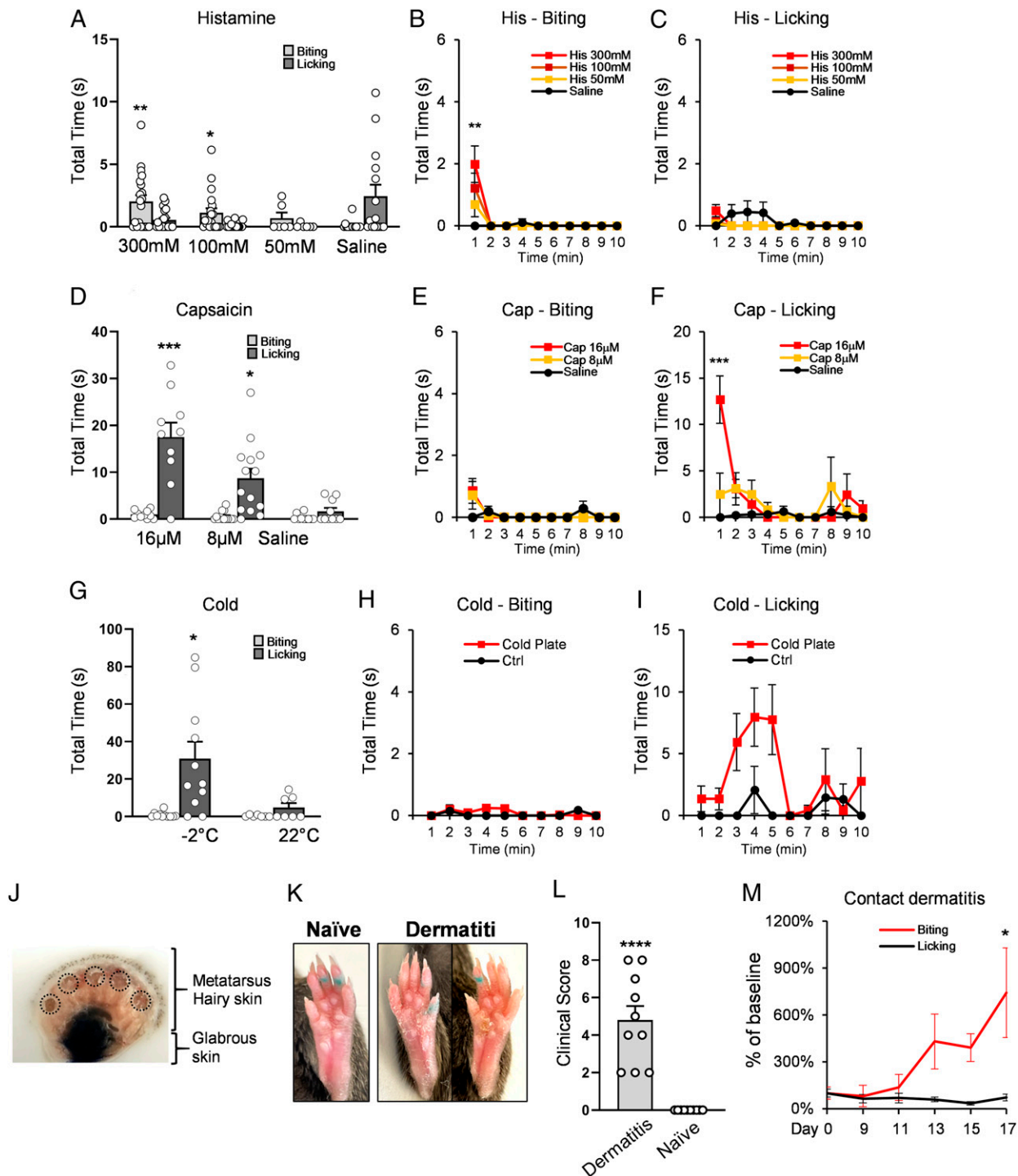


**Fig. 3.** Mice exhibit biting behavior in response to pruritogens in glabrous skin. (A) Histamine-induced dose-dependent biting behavior after glabrous skin injection ( $n = 6$  to  $20$  mice for each concentration). Data are nonparametric and analyzed using a Kruskal–Wallis test with Dunn’s post hoc test. (B and C) Histamine-induced biting (B) and licking (C) responses over time. Data are nonparametric and analyzed using a Kruskal–Wallis test. (D) Capsaicin-induced dose-dependent licking behavior after glabrous skin injection ( $n = 10$  to  $14$  mice for each concentration). Data are nonparametric and analyzed using a Kruskal–Wallis test with Dunn’s post hoc test. (E and F) Capsaicin-induced biting (E) and licking (F) responses over time. Data are nonparametric and analyzed using a Kruskal–Wallis test. (G) Cold-induced pain sensation evoked robust licking behavior, but not biting behavior ( $n = 7$  to  $12$  mice for each condition). Data are nonparametric and analyzed using a Mann–Whitney test. (H and I) Cold-induced biting (H) and licking (I) responses over time. Data are nonparametric and analyzed using a Mann–Whitney test. (J) Cross-section of a mouse plantar hindpaw showing trypan blue dye restricted in the glabrous skin side after the injection. (K) Images of hindpaws of WT mice treated with vehicle control or SADBE. Contact dermatitis in the plantar hindpaw is evidenced by the dryness and scabbing. (L) A clinical score was given for each paw (the sum of three 0-to-4 scores given for scabs, dryness, and redness). Data are nonparametric and analyzed using a Mann–Whitney test. (M) Percentage change in biting and licking behavior after contact dermatitis treatment in the plantar hindpaw. Dermatitis induced strong biting behaviors on day 17 and did not induce significant licking behaviors ( $n = 8$  mice in each group). Data are parametric and analyzed using a two-way ANOVA with Bonferroni post hoc. Data are presented as mean  $\pm$  SEM (\* $P < 0.05$ , \*\* $P < 0.01$ , \*\*\* $P < 0.001$ ).

was also observed, indicating the role of *MrgprC11*<sup>+</sup> neurons in glabrous skin pain sensation. Consistently, low concentrations of Bam8-22 (10  $\mu$ M and 50  $\mu$ M) injection into the plantar hindpaw of WT mice induced dose-dependent biting behavior. Significant licking behavior was observed from a high concentration of Bam8-22 (2 mM; Fig. 4 D–F). We did not observe any significant glabrous skin behavior after chloroquine or  $\beta$ -alanine injection (Fig. 4G).

**Ablation of *MrgprC11*<sup>+</sup> Neurons Reduces Itch in Glabrous Skin.** To examine if *MrgprC11*<sup>+</sup> neurons are required for pain and itch sensation in glabrous skin, we generated *MrgprC11*<sup>DTR</sup> mice to perform ablation of *MrgprC11*<sup>+</sup> neurons. A total of 77.8% of *MrgprC11*<sup>+</sup> neurons were ablated after diphtheria toxin (DTX) administration (16.3  $\pm$  0.11% in *ROSA26*<sup>DTR</sup> mice vs. 3.64  $\pm$  0.08% in *MrgprC11*<sup>DTR</sup> mice; SI Appendix, Fig. S5 A and B). Since about 27.7% of TRPV1<sup>+</sup> neurons express *MrgprC11*, the percentage of TRPV1<sup>+</sup> neurons was slightly reduced in *MrgprC11*<sup>DTR</sup> mice compared to the control mice. The majority of TRPV1<sup>+</sup> neurons are still intact, suggesting that the DTX treatment did not

induce any nonspecific neurotoxic effects (SI Appendix, Fig. S5 A and B). We first tested the sensitivity of *MrgprC11*<sup>DTR</sup> mice to potentially painful stimuli. *MrgprC11*<sup>DTR</sup> and *ROSA26*<sup>DTR</sup> mice showed similar thermal sensitivities as measured by hot plate, cold plate, and Hargreaves tests (SI Appendix, Fig. S5 C–E). Capsaicin injection into the glabrous hindpaw induced comparable licking behavior in both groups (SI Appendix, Fig. S5G). These results suggest that *MrgprC11*<sup>+</sup> neurons are not required for sensing thermal and chemical stimuli in glabrous skin. Both groups also exhibited equivalent threshold in response to von Frey filaments, suggesting that the ablation of *MrgprC11*<sup>+</sup> neurons did not affect mechanical sensitivity of the mice (SI Appendix, Fig. S5F).

We next compared the itch behavior between *MrgprC11*<sup>DTR</sup> and *ROSA26*<sup>DTR</sup> mice. We first injected histamine and Bam8-22 into the nape of the neck of the mice to examine their hairy skin itch sensation. The cell-ablated mice showed reduced scratching in response to both histamine and Bam8-22 (Fig. 4 H and I). We next examined the glabrous skin itch and found that ablation of *MrgprC11*<sup>+</sup> neurons did not affect histamine-induced biting, suggesting that *MrgprC11*<sup>+</sup> neurons are not required for histaminergic

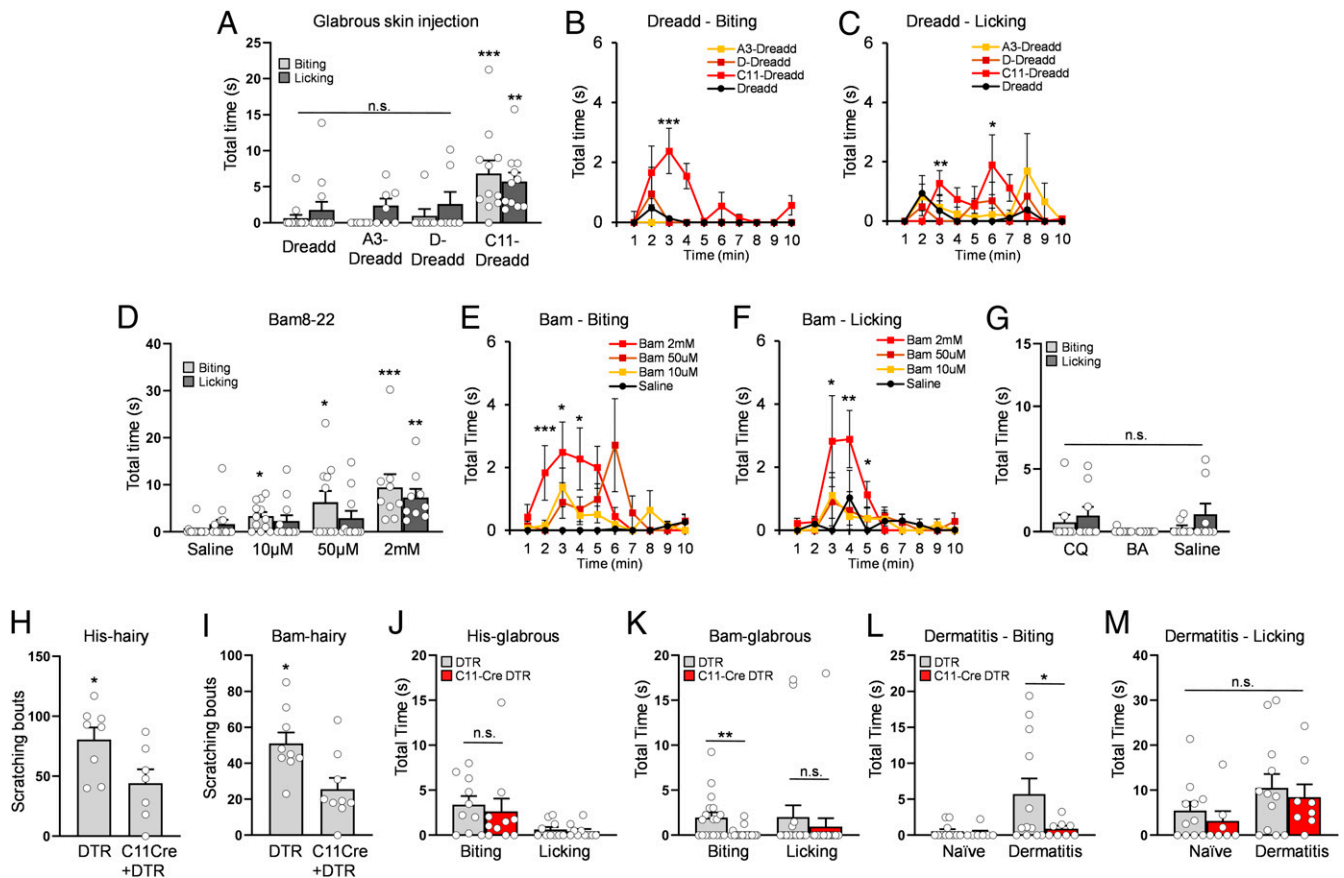


**Fig. 4.** *MrgprC11*<sup>+</sup> neurons mediate glabrous skin itch. (A) Chemogenetic activation of *MrgprC11*<sup>+</sup> nerve in the hindpaw glabrous skin (CNO, 0.2 mM, 4  $\mu$ L) induced significant biting and licking behavior. Activation of *MrgprA3*<sup>+</sup> and *MrgprD*<sup>+</sup> nerves did not induce significant glabrous skin behavior (CNO, 7.5 mM, 4  $\mu$ L;  $n = 8$  to 13 mice for each genotype). Data are nonparametric and analyzed using a Kruskal–Wallis test with Dunn’s post hoc. (B and C) Biting (B) and licking (C) responses in A over time. Data are nonparametric and analyzed using a Kruskal–Wallis test. (D) Low concentration of Bam8-22 (10  $\mu$ M and 50  $\mu$ M) induced specific biting, but not licking, after glabrous skin injection. A high concentration of Bam8-22 (2 mM) induced both biting and licking ( $n = 9$  to 11 mice for each group). Data are nonparametric and analyzed using a Kruskal–Wallis test with Dunn’s post hoc. (E and F) Bam8-22–induced biting (E) and licking (F) responses over time. Data are nonparametric and analyzed using a Kruskal–Wallis test. (G) High concentrations of chloroquine (12 mM) and  $\beta$ -alanine (300 mM) did not induce significant biting or licking ( $n = 8$  to 11 mice for each group). Data are nonparametric and analyzed using a Kruskal–Wallis test with Dunn’s post hoc. (H and I) Ablation of *MrgprC11*<sup>+</sup> neurons significantly decreased both histamine-induced (H) and Bam8-22–induced (I) biting in hairy skin ( $n = 7$  to 9 mice for each group). Data are parametric and analyzed using Welch’s  $t$  test. (J–K) Ablation of *MrgprC11*<sup>+</sup> neurons did not affect histamine-induced biting (J), but abolished Bam8-22–induced biting (K;  $n = 12$  to 18 mice for each group). Data are nonparametric and analyzed using a Mann–Whitney test. (L and M) Ablation of *MrgprC11*<sup>+</sup> neurons abolished biting behavior induced by contact dermatitis (L), but did not affect baseline licking (M;  $n = 10$  to 12 mice for each group). Data are parametric and analyzed using Welch’s  $t$  test. Data are presented as mean  $\pm$  SEM (\* $P < 0.05$ , \*\* $P < 0.01$ , \*\*\* $P < 0.001$ ). n.s., not statistically significant.

glabrous skin itch (Fig. 4J). However, the biting responses induced by Bam8-22 were almost lost in *MrgprC11<sup>DTR</sup>* mice compared to *ROSA26<sup>DTR</sup>* mice (Fig. 4K). Moreover, biting behavior induced by glabrous skin allergic contact dermatitis was almost abolished in the cell-ablated animals, suggesting that *MrgprC11<sup>+</sup>* neurons are required for glabrous skin chronic itch (Fig. 4L and M). In summary, our results demonstrate that *MrgprC11<sup>+</sup>* neurons are key mediators for both acute and chronic glabrous skin itch.

## Discussion

The mechanisms of hairy skin itch have been extensively studied. However, there are numerous dermatological conditions such as contact dermatitis, plantar and palmar psoriasis, tinea capitis, dyshidrosis, and cholestasis associated with glabrous skin itch (3–5, 39). Here, we present evidence showing that different mechanisms exist for hairy and glabrous skin itch. *MrgprA3<sup>+</sup>* and *MrgprD<sup>+</sup>* neurons mainly mediate hairy skin itch, whereas *MrgprC11<sup>+</sup>* neurons are key mediators for glabrous skin itch.

Both *MrgprA3<sup>+</sup>* and *MrgprD<sup>+</sup>* neurons are defined itch-sensing neurons for hairy skin (12, 18–20). Consistently, chemogenetic analysis from our current study and others showed that activation of *MrgprA3<sup>+</sup>* and *MrgprD<sup>+</sup>* nerves in the hairy skin (cheek and nape of the neck) induced robust scratching behavior (40, 41). However, *MrgprA3<sup>+</sup>* neurons sparsely innervate the glabrous skin and are unable to evoke glabrous skin behavior when directly stimulated using a chemogenetic approach or chloroquine. Therefore, we conclude that *MrgprA3<sup>+</sup>* neurons are not the main mediator for glabrous skin itch. Sharif et al. recently showed that optogenetic stimulation of *MrgprA3<sup>+</sup>* nerves in the plantar hindpaw triggered nocifensive behaviors including paw withdrawal, flinching, and licking (40). Optogenetic approach allows observation of immediately evoked behavioral responses without chemical injection and animal handling during the stimulation. *MrgprA3<sup>+</sup>* nerves in the glabrous skin, although sparse, may evoke transient nocifensive behaviors that can be easily missed during our hindpaw injection procedure.

Although *MrgprD<sup>+</sup>* neurons densely innervate the glabrous skin, they failed to produce any nocifensive behavioral responses after chemogenetic activation or  $\beta$ -alanine injection. This is in line with the previous studies suggesting that *MrgprD<sup>+</sup>* nerves in the plantar hindpaw mediate innocuous mechanical sensation (42–45). Optogenetic or chemogenetic activation of *MrgprD<sup>+</sup>* nerves in the plantar hindpaw evoked “nonpainful” withdrawal reflex of the hindpaw and did not induce pain sensation or aversive behavior. The different functional roles of *MrgprD<sup>+</sup>* neurons in hairy and glabrous skin support the hypothesis that different subtypes of DRG sensory neurons are recruited for itch in hairy skin and glabrous skin.

We observed dense *MrgprC11<sup>+</sup>* nerves in the glabrous skin of the mouse plantar hindpaw. *MrgprC11* agonist Bam8-22 directly excited 14.1% of sensory neurons innervating the glabrous skin. Activation of *MrgprC11<sup>+</sup>* nerves in the glabrous skin by either specific agonist Bam 8-22 or the chemogenetic approach produced robust biting responses. Moreover, ablation of *MrgprC11<sup>+</sup>* neurons almost abolished glabrous skin itch sensation induced by both Bam8-22 and allergic contact dermatitis. These results demonstrate that *MrgprC11<sup>+</sup>* neurons are key mediators for glabrous skin itch.

Ablation of *MrgprC11<sup>+</sup>* neurons significantly reduced histamine-induced itch in hairy skin, which is expected since histamine-sensitive neurons largely overlap with Bam8-22-sensitive neurons. However, loss of *MrgprC11<sup>+</sup>* neurons did not affect histamine-induced biting, indicating that different mechanisms exist mediating histaminergic itch in glabrous skin. These data present another example suggesting different itch mechanisms in hairy and glabrous skin. Histamine receptors are widely expressed in many cell types, including sensory neurons and resident skin cells such as keratinocytes and mast cells (46–48). Subcutaneous injection of

histamine can directly stimulate histamine-sensitive nerves to induce behavioral responses. It may also act upon resident skin cells, which in turn contribute to the activation of sensory nerves. Therefore, it is possible that ablation of *MrgprC11<sup>+</sup>* nerves in the glabrous skin inhibits the direct nerve stimulation by histamine, but did not block the indirect effects mediated by resident skin cells.

*MrgprC11* is expressed in ~18% of DRG neurons, which is a large and heterogeneous population. Although lower concentrations of Bam8-22 induced specific biting behavior, a high concentration of Bam8-22 also induced a slight increase of licking, suggesting that a subpopulation of *MrgprC11<sup>+</sup>* neurons can evoke pain sensation upon activation. Consistently, we observed both biting and licking behavior after chemogenetic activation of *MrgprC11<sup>+</sup>* nerves. Ablation of *MrgprC11<sup>+</sup>* neurons did not affect the thermal and mechanical sensitivities of the mice, suggesting that *MrgprC11<sup>+</sup>* neurons are not required for acute pain sensation. Indeed, the majority of TRPV1<sup>+</sup> neurons, the major pain mediator, were not affected by the ablation of *MrgprC11<sup>+</sup>* neurons.

Interestingly, *MrgprC11* labels almost all *MrgprA3<sup>+</sup>* neurons and most *Nppb<sup>+</sup>* neurons, suggesting that *MrgprC11<sup>+</sup>* neurons cover a large portion of the itch-sensing neurons in DRG that control both hairy and glabrous skin. It is likely that *MrgprA3<sup>+</sup>/MrgprC11<sup>+</sup>* neurons mediate hairy skin itch and *MrgprA3<sup>-</sup>/MrgprC11<sup>+</sup>* neurons mediate glabrous skin itch. Further investigations examining molecular and physiological differences between the *MrgprC11<sup>+</sup>* neurons innervating hairy and glabrous skin will provide insights into the mechanistic differences of itch in hairy and glabrous skin.

## Materials and Methods

**Animals.** All experiments were performed with approval from the Georgia Institute of Technology Animal Use and Care Committee. *MrgprA3<sup>GFP-Cre</sup>* (19, 24) and *Pirt<sup>GCaMP3</sup>* lines (28) were generated by previous studies. *MrgprD<sup>EGFP</sup>* knock-in line (24) and *MrgprC11<sup>CreERT2</sup>* BAC transgenic line was provided by Xinzhong Dong at the Johns Hopkins University (Baltimore, MD). *MrgprC11<sup>CreERT2</sup>* line was generated by the Gene Targeting & Transgenic Facility at Janelia Farm. Mice listed below were purchased from Jackson Laboratory: wild type C57BL/6 mice (stock no. 000664), *MrgprD<sup>CreERT2</sup>* (stock no. 031286), *ROSA26<sup>tdTomato</sup>* (stock no. 007909), and *ROSA26<sup>DREADD</sup>* (stock no. 026220). All mice used for these experiments have been backcrossed to C57BL/6 mice for at least 10 generations. All experiments were conducted using 2- to 4-mo-old (20 to 30 g) mice except mice used for Ca<sup>2+</sup> imaging assays, which were 4 to 5 wk old. Mice were housed in a vivarium with a 12-h light/dark cycle, housing groups of 5 maximum, with food/water ad libitum.

**Tamoxifen Treatments.** To specifically label *MrgprC11<sup>+</sup>* neurons, *MrgprC11<sup>CreERT2</sup>* mice were treated daily via oral gavage (22 g  $\times$  25 mm; FTP-22-25; Instech Laboratories) with 100 mg/kg of tamoxifen (T5648; Sigma) dissolved in sunflower seed oil (S5007; Sigma) for 5 d at 2 to 3 wk of age. To label *MrgprD<sup>+</sup>* neurons, *MrgprD<sup>CreERT2</sup>* mice were treated daily via oral gavage with 40 mg/kg of tamoxifen for 6 d at 5 to 6 wk of age (23). At least 1 wk was then given to drive recombination and reporter gene expression.

**Retrograde Tracing of Skin-Innervating Neurons.** Dil (0.2%, dissolved in 10% dimethyl sulfoxide and 90% saline; Invitrogen D3911) was injected into the skin of *Pirt<sup>GCaMP3</sup>* mice to retrogradely label skin-innervating neurons. Hindpaw plantar glabrous skin was injected to label glabrous-skin innervating neurons, and back hairy skin was injected to label hairy skin-innervating neurons. Lumbar (for glabrous skin) or thoracic (for hairy skin) DRGs were isolated for calcium imaging 1 wk after Dil injection. DRG sensory neurons were dissected, dissociated, and cultured on 8-mm glass coverslips. At 48 h after dissection, cells were imaged with calcium imaging buffer (NaCl 130 mM, KCl 3 mM, CaCl<sub>2</sub> 2.5 mM, MgCl<sub>2</sub> 0.6 mM, Hepes 10 mM, glucose 5 mM, NaHCO<sub>3</sub> 1.2 mM, pH 7.4, osmolarity 290 to 300 mOsm/kg) at 488-nm excitation to detect the fluorescent intensity level of GCaMP3. Chemicals were then applied to the cells by perfusion for 30 s, and a 20% increase in GCaMP3 fluorescence intensity was set as the threshold to identify responding cells. Chemicals used are listed as follows: chloroquine (Sigma PHR1258; 1 mM), Bam8-22 (custom-synthesized by Genscript; 1  $\mu$ M), and histamine (Sigma H7250; 20  $\mu$ M). Three mice were used for the analysis of each pruritogen.

**Immunostaining.** Immunohistochemistry staining was performed as previously described (19). Briefly, adult mice (8 to 12 wk old) were transcardially perfused with fixative (ice-cold 4% formaldehyde and 14% picric acid in phosphate-buffered saline solution). DRG, spinal cord, or skin were dissected, cryoprotected in 30% sucrose, and sectioned at a thickness of 20  $\mu\text{m}$ . Primary antibodies used were rabbit polyclonal anti-MrgprC11 (made by Proteintech Group; 1:500; validated in previous studies [49]), guinea pig anti-TRPV1 (Chemico ab5566; 1:500), chicken anti-GFP (Aves GFP-1010; 1:1,000), chicken anti-NF200 (Aves NFH; 1:1,000), rat anti-subP (Millipore MAB356; 1:500), rabbit anti-HA to detect hM3Dq expression (Cell Signaling Technologies 3724S; 1:500), goat anti-CGRP (Bio-Rad no. 1720-9007; 1:500), and rabbit anti-PK $\zeta$  (Santa Cruz Biotechnology sc-211; 1:2,000). Secondary antibodies used (all from Invitrogen and used at 1:500) were donkey anti-rabbit IgG-Alexa Fluor 555 (A-31572), goat anti-chicken IgY-Alexa Fluor 488 (A-11039), goat anti-guinea pig IgG-Alexa Fluor 488 (A-11073), donkey anti-rat IgG Alexa Fluor 488 (A-21208), goat anti-mouse IgG-Alexa Fluor 488 (A-11001), and donkey anti-rabbit IgG-Alexa Fluor 488 (A-11056). To detect IB4 binding, sections were incubated with 1:200 diluted IB4-Alexa 488 (I-21411; Invitrogen) during secondary antibody incubations.

**RNAscope In Situ Hybridization.** RNAscope in situ hybridization was performed using the RNAscope fluorescent multiplex kit (ACD no. 320850) according to the manufacturer's instructions. The following probes were used: MrgprA3 (no. 548161), MrgprC11 (no. 488771), MrgprD (no. 417921), Nppb (no. 425021), Lpar3 (no. 432591), Cyslr2 (no. 452621), and Dredd (hM3Dq; no. 407971).

Images for immunostaining and RNAscope in situ hybridization were acquired on a Zeiss LSM700 confocal microscope and analyzed in Fiji.

**Behavior Tests.** All experiments were performed with an experimenter blind to genotype using protocols approved by the animal care and use committee of Georgia Institute of Technology School of Biology. All behavior tests were performed from 8 AM to 1 PM in the light cycle in our animal facility. All mice were acclimated for 30 to 60 min to their testing environment the day before the behavioral tests.

**Back/cheek injections.** Behavioral assessment of hairy skin scratching behavior was performed as previously described (50). Briefly, mice were injected subcutaneously into the nape of the neck (50  $\mu\text{L}$ ) or the cheek (10  $\mu\text{L}$ ).

**Plantar glabrous skin injections.** A total of 4  $\mu\text{L}$  of chemicals was injected into the center of the planter hindpaw using custom-made 10  $\mu\text{L}$  Hamilton syringes with 30-gauge needles. The needle was inserted into the superficial glabrous skin area to limit the injected chemicals to the glabrous side of the paw. After the injection, the animal was immediately placed in a plastic cylinder on the clear acrylic platform. The behavioral responses were recorded using a single Sony HD camcorder (FDRAX33, 4K/24P) from a mirror underneath the clear platform to better visualize all behaviors directed to the hindpaw. The behavioral videos were analyzed in slow motion (0.25x normal speed) using Media Player Classic to differentiate behavioral responses. Chemicals used include histamine (Sigma H7250; 50 to 300 mM), capsaicin

(Sigma M2028; 8 to 16  $\mu\text{M}$ ), Bam8-22 (custom synthesized by Genscript; 10  $\mu\text{M}$  to 2 mM), and CNO (Cayman no. 16882; 0.2 to 7.5 mM).

**Cold plate to observe glabrous skin licking behavior.** The mice were placed in a plastic cylinder on the  $-2^\circ\text{C}$  cold plate for 2 min, and behavioral responses were recorded for analysis.

**Glabrous skin contact dermatitis.** Contact dermatitis was produced by treating the mice with the allergen SADBE (Sigma no. 339792; 0.5% in acetone), and the procedure included 7 d of the elicitation phase and 10 d of the induction phase. During the elicitation phase, 20  $\mu\text{L}$  of SADBE was applied to the shaved abdomen once a day for 3 d to initiate T lymphocyte sensitization. The induction phase started 1 wk after the first treatment on the abdomen. SADBE was applied to the plantar hindpaw skin once a day for 10 d to induce dermal inflammation. To limit dermatitis in the glabrous side of the paw, we only applied 2  $\mu\text{L}$  of SADBE to the plantar skin. Since SADBE is dissolved in acetone, which evaporates quickly after application, we rarely observed any SADBE solution flow to the hairy side of the paw. Clinical scores of the glabrous skin (summation of three scores, 0-4 for dryness, 0-4 for redness, and 0-4 for scabbing) were evaluated on day 17.

**Hot plate and cold plate for pain sensitivity.** Mice were placed inside a clear Plexiglas cylinder on a plate set at different temperatures (55  $^\circ\text{C}$  for hot plate and  $-2^\circ\text{C}$  for cold plate). The onset of brisk hindpaw lifts and/or flicking/licking of the hindpaw was assessed.

**Hargreaves test.** Mice were placed under a transparent plastic box (10  $\times$  5  $\times$  4.5 cm) on a glass floor, and infrared light was delivered to the hindpaw. The latency for the animal to withdraw its hindpaw was measured.

**von Frey filament test.** Mice were placed under a transparent plastic box on a metal mesh. von Frey filaments were applied to the hindpaw using the up/down method, and the threshold force corresponding to 50% withdrawal was determined.

**Statistical Analysis.** Data are presented as mean  $\pm$  SEM. GraphPad Prism scientific software version 9.0.0 was used for statistical analysis. Statistical significance was determined using both nonparametric (Mann-Whitney, Kruskal-Wallis test with Dunn's multiple-comparisons post hoc test or  $\chi^2$  test) and parametric methods (Welch's *t* test, one-way ANOVA with post hoc, or two-way ANOVA with Bonferroni post hoc analysis) due to differences in the normality and sample size of the data. The specific tests used to analyze each data set is indicated within the individual figure legends. Differences were considered as statistically significant at a value of  $P < 0.05$ ,  $P < 0.01$ ,  $P < 0.001$ , or  $P < 0.0001$ .

**Data Availability.** All study data are included in the article and/or supporting information.

**ACKNOWLEDGMENTS.** We thank the animal facility at Georgia Institute of Technology for the animal care and services. This work was supported by grants from the US NIH (NS087088 and HL141269) and Pfizer Aspire Dermatology Award to L.H.

1. G. Yosipovitch, J. D. Bernhard, Clinical practice. Chronic pruritus. *N. Engl. J. Med.* **368**, 1625–1634 (2013).
2. A. Ikoma, M. Steinhoff, S. Ständer, G. Yosipovitch, M. Schmelz, The neurobiology of itch. *Nat. Rev. Neurosci.* **7**, 535–547 (2006).
3. U. Beuers, A. E. Kremer, R. Bolier, R. P. Elferink, Pruritus in cholestasis: Facts and fiction. *Hepatology* **60**, 399–407 (2014).
4. A. M. Brunasso *et al.*, Clinical and epidemiological comparison of patients affected by palmoplantar plaque psoriasis and palmoplantar pustulosis: A case series study. *Br. J. Dermatol.* **168**, 1243–1251 (2013).
5. S. M. Lofgren, E. M. Warshaw, Dyshidrosis: Epidemiology, clinical characteristics, and therapy. *Dermatitis* **17**, 165–181 (2006).
6. X. Dong, X. Dong, Peripheral and central mechanisms of itch. *Neuron* **98**, 482–494 (2018).
7. R. H. LaMotte, S. G. Shimada, P. Sikand, Mouse models of acute, chemical itch and pain in humans. *Exp. Dermatol.* **20**, 778–782 (2011).
8. J. E. Swett, C. J. Woolf, The somatotopic organization of primary afferent terminals in the superficial laminae of the dorsal horn of the rat spinal cord. *J. Comp. Neurol.* **231**, 66–77 (1985).
9. J. H. Kaas, "Somatosensory system" in *The Human Nervous System*, J. K. Mai, G. Paxinos, Eds. (Academic Press, ed. 3, 2012), pp. 1074–1109.
10. C. L. Li *et al.*, Somatosensory neuron types identified by high-coverage single-cell RNA-sequencing and functional heterogeneity. *Cell Res.* **26**, 83–102 (2016).
11. G. Hu *et al.*, Single-cell RNA-seq reveals distinct injury responses in different types of DRG sensory neurons. *Sci. Rep.* **6**, 31851 (2016).
12. D. Usoskin *et al.*, Unbiased classification of sensory neuron types by large-scale single-cell RNA sequencing. *Nat. Neurosci.* **18**, 145–153 (2015).
13. N. Sharma *et al.*, The emergence of transcriptional identity in somatosensory neurons. *Nature* **577**, 392–398 (2020).
14. Y. Zheng *et al.*, Deep sequencing of somatosensory neurons reveals molecular determinants of intrinsic physiological properties. *Neuron* **103**, 598–616.e7 (2019).
15. X. Dong, S. Han, M. J. Zylka, M. I. Simon, D. J. Anderson, A diverse family of GPCRs expressed in specific subsets of nociceptive sensory neurons. *Cell* **106**, 619–632 (2001).
16. L. Qu *et al.*, Enhanced excitability of MRGPRA3- and MRGPRD-positive nociceptors in a model of inflammatory itch and pain. *Brain* **137**, 1039–1050 (2014).
17. Y. Zhu, C. E. Hanson, Q. Liu, L. Han, Mrgprs activation is required for chronic itch conditions in mice. *Itch (Phila.)* **2**, e9 (2017).
18. Q. Liu *et al.*, Sensory neuron-specific GPCR Mrgprs are itch receptors mediating chloroquine-induced pruritus. *Cell* **139**, 1353–1365 (2009).
19. L. Han *et al.*, A subpopulation of nociceptors specifically linked to itch. *Nat. Neurosci.* **16**, 174–182 (2013).
20. Q. Liu *et al.*, Mechanisms of itch evoked by  $\beta$ -alanine. *J. Neurosci.* **32**, 14532–14537 (2012).
21. H. J. Solinski *et al.*, Nppb neurons are sensors of mast cell-induced itch. *Cell Rep.* **26**, 3561–3573.e4 (2019).
22. W. Olson *et al.*, Sparse genetic tracing reveals regionally specific functional organization of mammalian nociceptors. *eLife* **6**, e29507 (2017).
23. Y. Xing *et al.*, Visualizing the itch-sensing skin arbors. *BioRxiv* [Preprint] (2020). <https://doi.org/10.1101/2020.05.18.098871>.
24. M. J. Zylka, F. L. Rice, D. J. Anderson, Topographically distinct epidermal nociceptive circuits revealed by axonal tracers targeted to MrgprD. *Neuron* **45**, 17–25 (2005).
25. H. R. Koerber, P. B. Brown, Somatotopic organization of hindlimb cutaneous nerve projections to cat dorsal horn. *J. Neurophysiol.* **48**, 481–489 (1982).
26. C. Molander, G. Grant, Cutaneous projections from the rat hindlimb foot to the substantia gelatinosa of the spinal cord studied by transganglionic transport of WGA-HRP conjugate. *J. Comp. Neurol.* **237**, 476–484 (1985).

27. C. J. Woolf, M. Fitzgerald, Somatotopic organization of cutaneous afferent terminals and dorsal horn neuronal receptive fields in the superficial and deep laminae of the rat lumbar spinal cord. *J. Comp. Neurol.* **251**, 517–531 (1986).
28. Y. S. Kim *et al.*, Central terminal sensitization of TRPV1 by descending serotonergic facilitation modulates chronic pain. *Neuron* **81**, 873–887 (2014).
29. J. Meixiong, C. Vasavda, S. H. Snyder, X. Dong, MRGPRX4 is a G protein-coupled receptor activated by bile acids that may contribute to cholestatic pruritus. *Proc. Natl. Acad. Sci. U.S.A.* **116**, 10525–10530 (2019).
30. Y. Liu *et al.*, Mechanisms of compartmentalized expression of Mrg class G-protein-coupled sensory receptors. *J. Neurosci.* **28**, 125–132 (2008).
31. H. Wheeler-Aceto, F. Porreca, A. Cowan, The rat paw formalin test: Comparison of noxious agents. *Pain* **40**, 229–238 (1990).
32. H. Wheeler-Aceto, A. Cowan, Standardization of the rat paw formalin test for the evaluation of analgesics. *Psychopharmacology (Berl.)* **104**, 35–44 (1991).
33. J. R. Deuis, L. S. Dvorakova, I. Vetter, Methods used to evaluate pain behaviors in rodents. *Front. Mol. Neurosci.* **10**, 284 (2017).
34. N. Imamachi *et al.*, TRPV1-expressing primary afferents generate behavioral responses to pruritogens via multiple mechanisms. *Proc. Natl. Acad. Sci. U.S.A.* **106**, 11330–11335 (2009).
35. T. Akiyama, M. I. Carstens, E. Carstens, Spontaneous itch in the absence of hyperalgesia in a mouse hindpaw dry skin model. *Neurosci. Lett.* **484**, 62–65 (2010).
36. H. Nojima, J. M. Cuellar, C. T. Simons, M. I. Carstens, E. Carstens, Spinal c-fos expression associated with spontaneous biting in a mouse model of dry skin pruritus. *Neurosci. Lett.* **361**, 79–82 (2004).
37. K. Hagiwara, H. Nojima, Y. Kuraishi, Serotonin-induced biting of the hind paw is itch-related response in mice. *Pain Res.* **14**, 53–59 (1999).
38. A. E. Scott, M. L. Kashion, B. Yucesoy, M. I. Luster, S. S. Tinkle, Insights into the quantitative relationship between sensitization and challenge for allergic contact dermatitis reactions. *Toxicol. Appl. Pharmacol.* **183**, 66–70 (2002).
39. S. Ali, T. A. Graham, S. E. Forgie, The assessment and management of tinea capitis in children. *Pediatr. Emerg. Care* **23**, 662–665, quiz 666–668 (2007).
40. B. Sharif, A. R. Ase, A. Ribeiro-da-Silva, P. Séguéla, Differential coding of itch and pain by a subpopulation of primary afferent neurons. *Neuron* **106**, 940–951.e4 (2020).
41. S. Sun *et al.*, Leaky gate model: Intensity-dependent coding of pain and itch in the spinal cord. *Neuron* **93**, 840–853.e5 (2017).
42. I. Abdus-Saboor *et al.*, Development of a mouse pain scale using sub-second behavioral mapping and statistical modeling. *Cell Rep.* **28**, 1623–1634.e4 (2019).
43. S. Vrontou, A. M. Wong, K. K. Rau, H. R. Koerber, D. J. Anderson, Genetic identification of C fibres that detect massage-like stroking of hairy skin in vivo. *Nature* **493**, 669–673 (2013).
44. H. Beaudry, I. Daou, A. R. Ase, A. Ribeiro-da-Silva, P. Séguéla, Distinct behavioral responses evoked by selective optogenetic stimulation of the major TRPV1+ and MrgD+ subsets of C-fibers. *Pain* **158**, 2329–2339 (2017).
45. T. Huang *et al.*, Identifying the pathways required for coping behaviours associated with sustained pain. *Nature* **565**, 86–90 (2019).
46. E. B. Thangam *et al.*, The role of histamine and histamine receptors in mast cell-mediated allergy and inflammation: The hunt for new therapeutic targets. *Front. Immunol.* **9**, 1873 (2018).
47. K. Schaper-Gerhardt *et al.*, The role of the histamine H<sub>4</sub> receptor in atopic dermatitis and psoriasis. *Br. J. Pharmacol.* **177**, 490–502 (2020).
48. K. E. Cannon *et al.*, Immunohistochemical localization of histamine H<sub>3</sub> receptors in rodent skin, dorsal root ganglia, superior cervical ganglia, and spinal cord: Potential antinociceptive targets. *Pain* **129**, 76–92 (2007).
49. L. Han *et al.*, Mrgprs on vagal sensory neurons contribute to bronchoconstriction and airway hyper-responsiveness. *Nat. Neurosci.* **21**, 324–328 (2018).
50. S. G. Shimada, R. H. LaMotte, Behavioral differentiation between itch and pain in mouse. *Pain* **139**, 681–687 (2008).

## **Supplementary Information for**

### **MrgprC11<sup>+</sup> sensory neurons mediate glabrous skin itch**

Haley R. Steele, Yanyan Xing, Yuyan Zhu, Henry B. Hilley, Katy Lawson, Yeseul Nho, Taylor Niehoff, Liang Han\*

School of Biological Sciences, Georgia Institute of Technology, Atlanta, GA 30332, United States

\*Corresponding author: Liang Han, PhD, School of Biological Sciences, Georgia Institute of Technology, Atlanta, GA 30332, USA. Email: [liang.han@biology.gatech.edu](mailto:liang.han@biology.gatech.edu)

#### **This PDF file includes:**

Legends for Movie S1-S4

Figures S1 to S5

**Movie S1**

Short video showing biting behavior at 0.25X speed.

**Movie S2**

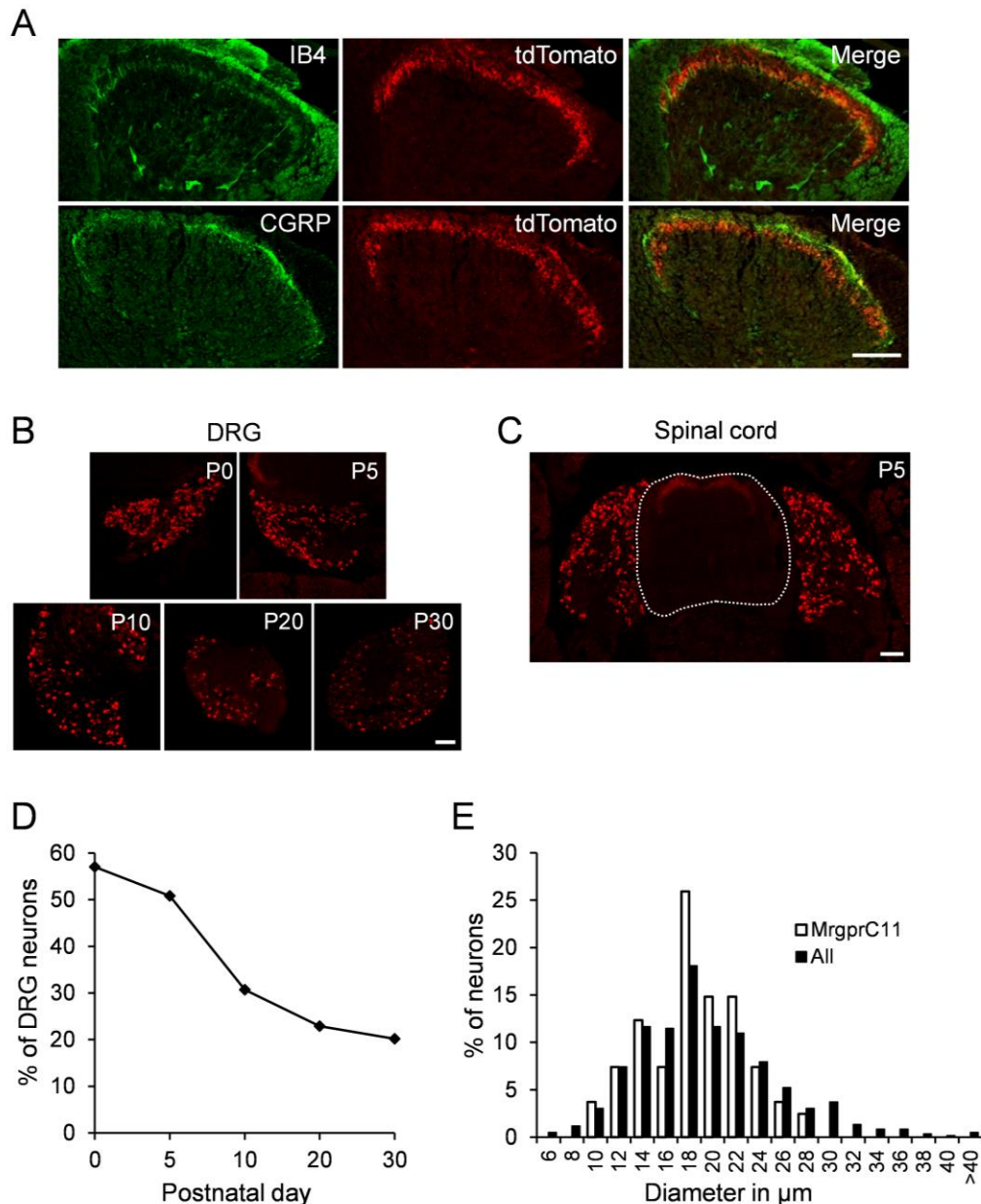
Short video showing licking behavior at 0.25X speed.

**Movie S3**

Longer video showing mouse behaviors in one minute. Three different biting episodes induced by Bam8-22 were slowed down to 0.25X speed and other parts of the video were played at 2X speed.

**Movie S4**

Longer video showing mouse behaviors in one minute. A single licking episode induced by capsaicin was slowed down to 0.25X speed and other parts of the video were played at 2X speed.



**Supplemental Figure 1. Characterization of MrgprC11<sup>+</sup> neurons, related to Figure 1.**

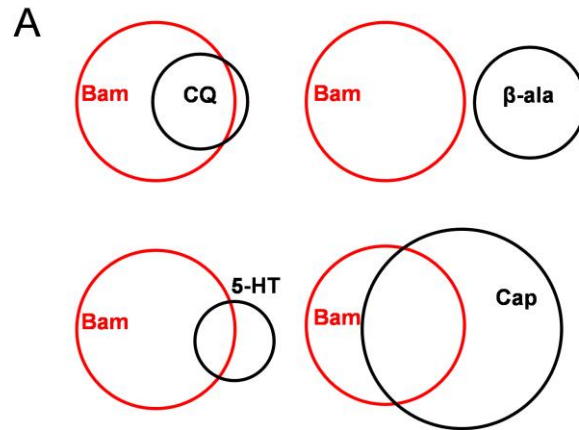
(A) Spinal cord cross-sections from the thoracic region of adult *MrgprC11<sup>CreERT2</sup>; ROSA26<sup>tdTomato</sup>* mice labeled with IB4 or CGRP (green). MrgprC11<sup>+</sup> axons, visualized by tdTomato fluorescence, co-terminated with IB4<sup>+</sup> fibers in the spinal lamina II<sub>middle</sub>, dorsal of PKCγ lamina and ventral to CGRP<sup>+</sup> lamina. Scale bar represents 100 μm.

(B) Lumbar DRG sections from WT mice at different ages. The percentage of MrgprC11<sup>+</sup> neurons declines while the mice age. Scale bar represents 100 μm.

(C) A lumbar spinal cord section from a P5 mouse labeled with MrgprC11 antibody. MrgprC11 is highly expressed in the DRG and is absent from the spinal cord except for central DRG terminal innervation in the dorsal horn. Scale bar represents 100 μm.

(D) The percentage of MrgprC11<sup>+</sup> DRG neurons by age.

(E) The percentage of MrgprC11<sup>+</sup> neurons in adult mice by size compared to all DRG neurons.



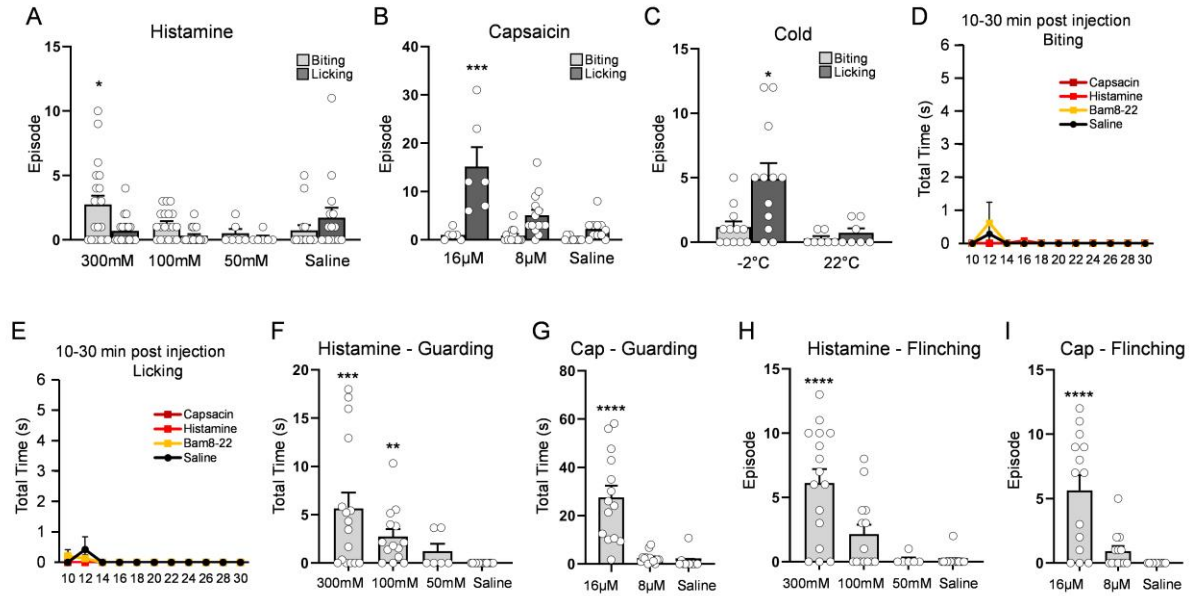
**B** Calcium imaging analysis of MrgprC11<sup>+</sup> sensory neurons

	% responded to Bam8-22
CQ-sensitive	89.6% (121/135)
$\beta$ -alanine-sensitive	0% (0/172)
5-HT-sensitive	48.3% (45/93)
Capsaicin-sensitive	43.6% (146/335)

**Supplemental Figure 2. Calcium imaging analysis of MrgprC11<sup>+</sup> neurons.**

(A) DRG sensory neurons isolated from *Pirt<sup>GCaMP3</sup>* mice were challenged with Bam8-22 (1  $\mu$ M) first, and then one of the four chemicals listed: CQ (1 mM),  $\beta$ -alanine (1 mM), 5-HT (100  $\mu$ M), and Capsaicin (1  $\mu$ M). Venn Diagrams illustrating the overlapping patterns. The sizes of the circles are proportional to the percentages of neurons responded.

(B) Table showing percentages of CQ,  $\beta$ -alanine, 5-HT, or Capsaicin-sensitive neurons that responded to Bam8-22. The numbers of neurons analyzed are shown in parenthesis. Cells from 4 mice were pooled together for analysis of each chemical.



**Supplemental Figure 3. Mice exhibit biting behaviors in response to pruritogens in glabrous skin.**

(A-C) Episode data for the histamine, capsaicin, and cold plate-induced behavior tests respectively. Episode data is consistent with total time data shown in Figure 3. (A) Histamine induced significant biting after glabrous skin injection. (B) Capsaicin induced dose-dependent licking after glabrous skin injection. (C) Cold-induced pain sensation evoked robust licking behavior, but not biting behavior. N numbers are the same as shown in main Figure 3.

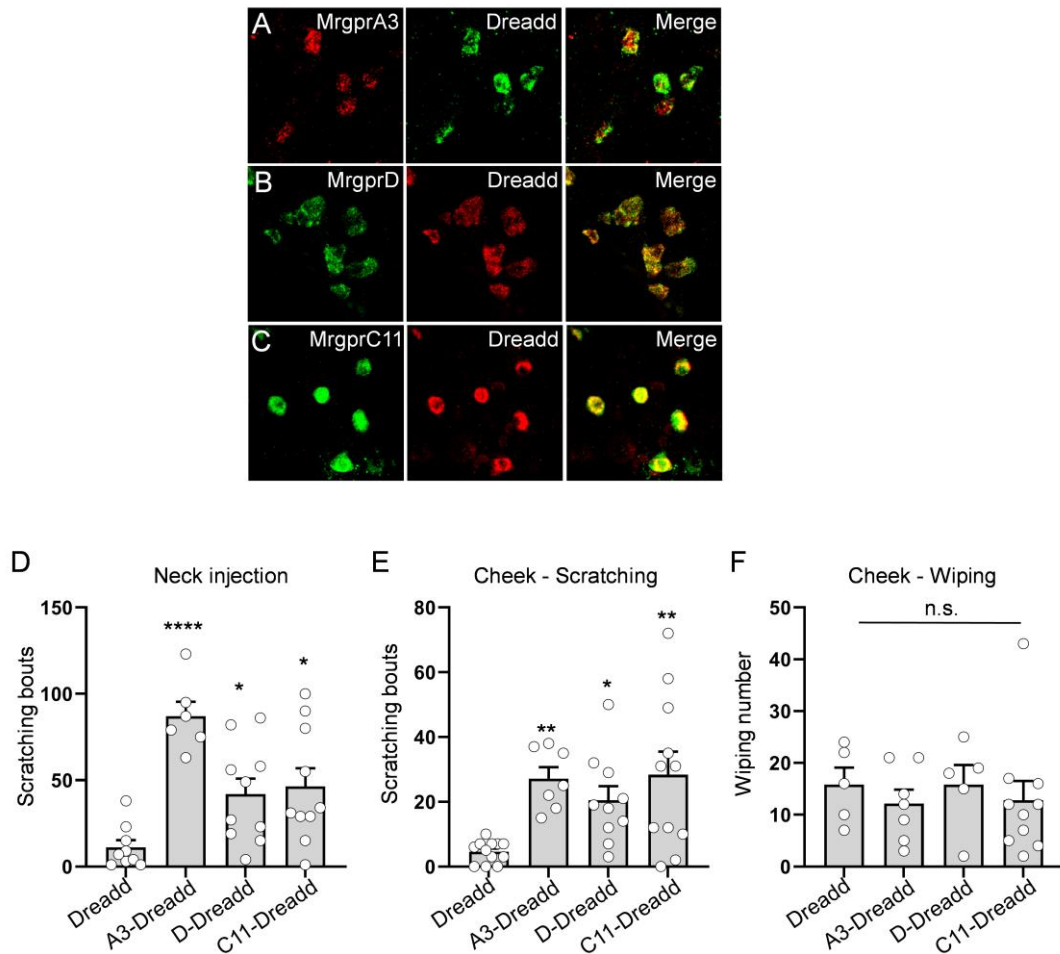
(D-E) 10-30 minutes post injection mice exhibited no major behavioral responses to Capsaicin, Histamine, or Bam8-22 compared to Saline control. N = 6 mice for each group.

(F-G) Both histamine and capsaicin induced guarding (lifting of the paw and holding it above the platform without licking or biting). N = 6 mice for each group.

(H-I) Both histamine and capsaicin induced flinching (rapid shaking of the hindpaw).

N numbers are the same as shown in main Figure 3.

Data are represented as mean  $\pm$  SEM. Data for all figures (A-I) are non-parametric and (A-B, D-I) were analyzed using Kruskal-Wallis tests with Dunn's post-hoc. Figure C was analyzed using a Mann-Whitney test. \* $p < 0.05$ , \*\* $p < 0.01$ , \*\*\* $p < 0.001$ .



### Supplemental Figure 4. Activation of MrgprA3<sup>+</sup>, MrgprD<sup>+</sup> and MrgprC11<sup>+</sup> nerve in the hairy skin induce itch

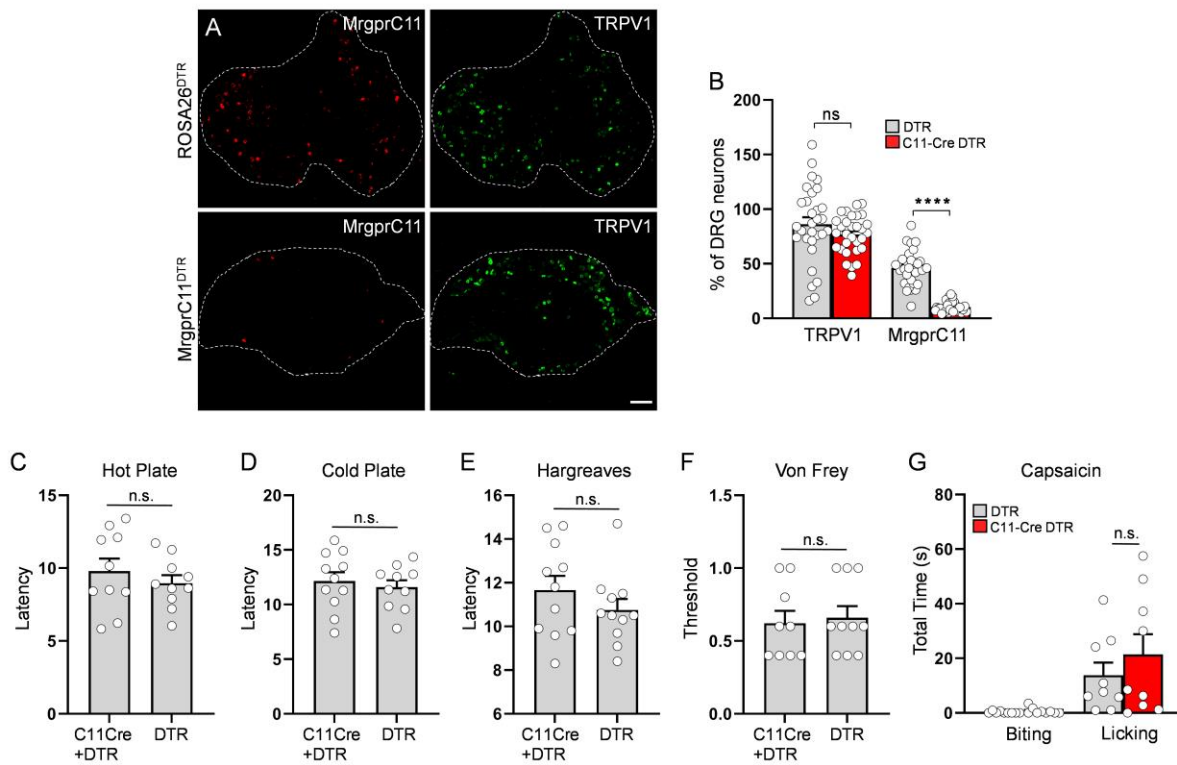
(A-B) RNAscope fluorescent *in situ* hybridization of lumbar DRG sections collected from adult *MrgprA3*<sup>GFP-Cre</sup>; *ROSA26*<sup>DREADD</sup> (A) and *MrgprD*<sup>CreERT2</sup>; *ROSA26*<sup>DREADD</sup> (B) mice detecting the indicated markers. DREADD was faithfully expressed in both MrgprA3<sup>+</sup> (A) and MrgprD<sup>+</sup> (B) neurons.

(C) Immunostaining of lumbar DRG sections collected from adult *MrgprC11*<sup>CreERT2</sup>; *ROSA26*<sup>DREADD</sup> mice using MrgprC11 antibody and GFP antibody. The hM3Dq transgene in *ROSA26*<sup>DREADD</sup> mice was fused with mCitrine that can be detected by GFP antibody.

(D) Chemogenetic activation of MrgprA3<sup>+</sup>, MrgprC11<sup>+</sup>, and MrgprD<sup>+</sup> nerves in the back hairy skin (CNO, 7.5 mM, 50 μl) induced scratching behaviors. N = 6-10 mice for each genotype.

(E-F) Chemogenetic activation of MrgprA3<sup>+</sup>, MrgprC11<sup>+</sup>, and MrgprD<sup>+</sup> nerves in the cheek hairy skin (CNO, 7.5 mM, 10 μl) induced scratching behaviors (E), and did not induce wiping behavior (F). N = 5-11 mice for each genotype.

All data (D-F) are parametric and analyzed with a one-way ANOVA with post-hoc test. Data are represented as mean ± SEM. \*p < 0.05, \*\*p < 0.01, \*\*\*p < 0.001. n.s.: not statistically significant.



### Supplemental Figure 5. Ablation of *MrgprC11*<sup>+</sup> neurons did not affect acute pain

(A) Immunostaining of lumbar DRG sections collected from DTX-treated *MrgprC11*<sup>CreERT2</sup>; *ROSA26*<sup>DTR</sup> and *ROSA26*<sup>DTR</sup> control mice. 77.8% of *MrgprC11*<sup>+</sup> neurons were ablated after DTX treatments. Scale bar represents 100  $\mu$ m.

(B) Percentage of *MrgprC11*<sup>+</sup> and TRPV1<sup>+</sup> neurons in DRG after DTX treatments.

(C-F) Ablation of *MrgprC11*<sup>+</sup> neurons did not affect pain sensitivity. DTX-treated *MrgprC11*<sup>CreERT2</sup>; *ROSA26*<sup>DTR</sup> and *ROSA26*<sup>DTR</sup> mice exhibited comparable thermal sensitivity measured by the hot plate (55°C) (C), cold plate (0°C) (D), and Hargreaves tests (E). Both groups showed similar mechanical sensitivity measured by von Frey test (F). N = 9-11 mice for each group.

(G) Ablation of *MrgprC11*<sup>+</sup> neurons did not affect capsaicin-induced licking. N = 9 mice for each group.

Data are presented as mean  $\pm$  SEM. All data (B-F) are parametric and analyzed using Welch's t-test. Data (G) are nonparametric and analyzed using a Mann-Whitney test. \*\*\*\*p < 0.0001. n.s.: not statistically significant.